Article

Fabrication of Nanoscale Metallic Spirals Using Phospholipid Microtubule Organizational Templates

Ronald R. Price, Walter J. Dressick, and Alok Singh

J. Am. Chem. Soc., **2003**, 125 (37), 11259-11263• DOI: 10.1021/ja036173g • Publication Date (Web): 15 August 2003

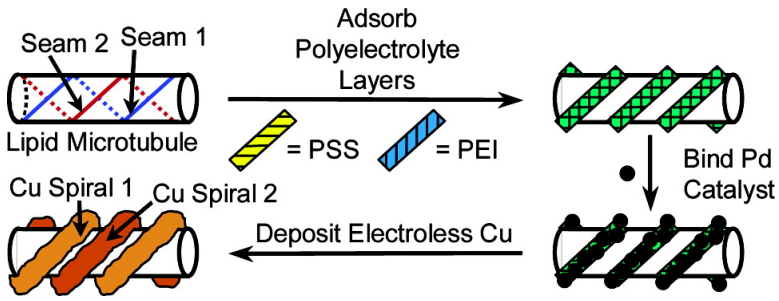

More About This Article

Additional resources and features associated with this article are available within the HTML version:

- Supporting Information
- Links to the 13 articles that cite this article, as of the time of this article download
- Access to high resolution figures
- Links to articles and content related to this article
- Copyright permission to reproduce figures and/or text from this article

View the Full Text HTML

J|A|C|S
ARTICLES
Published on Web 08/15/2003

Fabrication of Nanoscale Metallic Spirals Using Phospholipid Microtubule Organizational Templates

Ronald R. Price,* Walter J. Dressick, and Alok Singh

Contribution from the Naval Research Laboratory, Center for Bio/Molecular Science and Engineering, Code 6900, 4555 Overlook Avenue, SW, Washington, D.C. 20375

Received May 15, 2003; E-mail: rrp@cbmse.nrl.navy.mil

Abstract: We describe the fabrication of metallic Cu spiral/helical nanostructures prepared via selective electroless metallization of a phospholipid microtubule template. The metallization template is created through selective, sequential adsorption of the oppositely charged polyelectrolytes, sodium poly(styrenesulfonate) (PSS) and poly(ethyleneimine) (PEI), onto nanoscale seams naturally occurring on the microtubule surface. A negatively charged Pd(II) nanoparticle catalyst is bound to the terminal cationic PEI layer of the multilayer film and initiates selective template metallization to form the helical Cu nanostructures. Details of the process are presented, and a mechanism and factors affecting the control of the feature critical dimensions are discussed.

Introduction

The manufacture of "microelectromechanical systems" (MEMS) refers to the fabrication of sensors, actuators, and various other devices having at least some of their component dimensions in the micrometer range.[1] Currently such devices are produced using standard micromanufacturing methods, including lithography, materials deposition (e.g., CVD, sputtering, or laser deposition), wet bulk or surface micromachining, or micromolding, alone or in combination. However, as device dimensions shrink toward nanoscale size regimes, decreases in manufacturing accuracy with feature size associated with use of these methods will require development of new manufacturing process techniques.[2] To facilitate the fabrication of these smaller devices, there has been an increasing interest in the development of molecular materials that can self-assemble in solution to form unique microscale structures useful as templates for device manufacture. This biomimetic approach borrows from nature, which routinely fabricates a range of complex microscopic structures (e.g., cells or diatom shells) having nanoscale internal features from simpler materials such as amino acids, metal ions, and lipids.[3,4] In this Article, we apply this general concept to exploit spiral seam features of self-assembled diacetylenic phospholipid microtubules as templates for the preparation of nanoscale metal coils using an electroless (EL) metallization approach. The metal spiral structures so formed are potentially useful as springs or inductors for MEMS devices and interlocking reinforcements for composite materials.

Experimental Section

Materials. Deionized H_2O (18 MΩ cm) was used for all of the work. All materials were from Aldrich Chemicals (Milwaukee, WI) except (L)-1,2-bis-(tricosa-10,12-diynoyl)-*sn*-glycero-3-phosphocholine ($DC_{8,9}$PC; JP Laboratories, Princeton, NJ), MeOH and EtOH (Fisher Scientific, Pittsburgh, PA), and Cuposit 44 EL Cu bath (Shipley Co., Marlborough, MA). All materials were used as received. (L)-1,2-Bis-(tricosa-10,12-diynoyl)-*sn*-glycero-3-phosphoethanol lipid ($DC_{8,9}$PEOH; H^+ form) was prepared according to the literature method.[5,6]

Formation of Tubules. Lipid (3.12 mg/mL; pure $DC_{8,9}$PC or a 2 wt % $DC_{8,9}$PEOH/$DC_{8,9}$PC mixture) was dissolved in a 4:1 v/v MeOH/EtOH solution at 55 °C. To 4 volumes of this solution was added 1 volume of H_2O preheated to 55 °C, and the resulting solution was cooled to ∼20 °C at <5 °C h^{-1}. The tubules (lengths ∼10−90 μm; diameters ∼0.45−0.50 μm) formed were dialyzed (50 000 MW cutoff tube; Spectropore dialysis tubes) against 0.2 M HCl for 24 h to remove the alcohol, collected by centrifugation (5000*g*, 20 min), and resuspended in an equivalent volume of H_2O.

Polyelectrolyte Depositions. Aqueous solutions of poly(ethyleneimine) (PEI, MW 40 000) and sodium poly(styrenesulfonate) (PSS, MW 60 000) were separately prepared at concentrations of ∼0.25 mg/mL each. These polyelectrolyte concentrations and the solution volumes required for complete adsorption to the tubules were determined by independent titration of tubules with polyelectrolyte using indicator dyes as follows: An aqueous tubule suspension (∼2 mg/mL) was treated with (cationic) Nile Blue dye until the supernatant exhibited a persistent blue color, signifying completion of dye adsorption by the tubule defect sites. The tubules were isolated by centrifugation and resuspended in an equivalent volume of water. No desorption of dye from the tubules into the water was observed. Aliquots of PEI solution were added by micropipet to the tubule suspension, and the supernatant became blue in color as PEI displaced the adsorbed dye. When no further supernatant color change was noted (UV−visible spectroscopy), the effective amount of PEI needed for adsorption was calculated from the concentration and volume of the PEI solution added. A small amount of dye remained bound on the tubule, presumably that portion bound on the walls or trapped within the PEI layer during its adsorption. The titration of the tubules using (anionic) Congo Red dye and PSS solution to determine the quantity of PSS needed for multilayer formation proceeded similarly.

(1) Madou, M. J. *Fundamentals of Microfabrication: The Science of Miniaturization*, 2nd ed.; CRC Press: New York, 2002; Chapter 1.
(2) Evans, C. *Precision Engineering: An Evolutionary View*; Cranfield Press: Bedford, England, 1989; and references therein.
(3) Ball, P. *Nanotechnology* **2002**, *13*, R15.
(4) Simpson, T. L.; Volcani, B. E. In *Silicon and Siliceous Structures in Biological Systems*; Simpson, T. L., Volcani, B. E., Eds.; Springer-Verlag: New York, 1981; Chapter 1 and references therein.
(5) Markowitz, M.; Singh, A. *Langmuir* **1991**, *7*, 16.
(6) Singh, A. U.S. Patent 5,441,876, 1995.

Polyelectrolyte depositions were performed by adding the PSS solution[7] to the $DC_{8,9}PC$ tubule suspension in a 1:1 v/v ratio and allowing the mixture to stand for 30 min. Thereafter, volumes of PEI, PSS, and PEI solutions equivalent to the initial volume of the tubule suspension were sequentially added in 30 min intervals. The tubules were then centrifuged (5000*g*, 10 min) and resuspended in H_2O. For the mixed lipid 2 wt % $DC_{8,9}PEOH/DC_{8,9}PC$ tubules, the procedure was identical except for the following two changes: (1) PEI rather than PSS solution was used for the first treatment,[7] and (2) a three-layer polyelectrolyte film comprising PEI, PSS, and a terminal PEI layer was applied.[8]

Metal Deposition. PD1 catalyst was prepared using the literature method,[9] and **PD3** was prepared as follows: 60 mg of $Na_2PdCl_4 \cdot 3H_2O$ was completely dissolved in 1 mL of 1.00 M NaCl (aq) solution in a 50 mL volumetric flask. A 10 mL aliquot of 0.10 M morpholinoethane sulfonate pH 5 buffer was added, and the flask was diluted to the mark with H_2O. The flask was allowed to stand for 20 h in a water bath (24 $\pm$ 1 °C). A 5 mL aliquot of the resulting dispersion was then removed and discarded. The flask was diluted to the mark with 1.00 M NaCl (aq) solution once again to complete the preparation of the **PD3** catalyst dispersion, which was used within 1 week after preparation. **PD1** or **PD3** was added to the aqueous tubule suspension (~2.5 mg/mL) in a 1:1 v/v catalyst/tubule dispersion ratio. After 15 min, the tubules were separated from the catalyst supernatant by centrifugation as above and resuspended in H_2O. Cuposit 44 EL Cu bath was added to the tubule suspension in a 2.5:1 v/v EL Cu/tubule dispersion ratio, and the metallization was allowed to proceed for various times at room temperature. The spiral metal nanostructures formed were isolated by centrifugation to remove salts, resuspended in H_2O, and recentrifuged. The metal spirals were finally resuspended in EtOH (~40 °C) to extract the lipid and collected by filtration or centrifugation. During examination by SEM, the spiral structures were analyzed by energy-dispersive X-ray microanalysis to confirm the identity of the deposited material as Cu metal. Cu feature dimensions were measured from SEM photographs using a literature procedure,[10] and pitch angles were determined from the distance traversed by one complete turn of a Cu spiral (measured from the centers of the Cu wire deposits) and the feature diameter. Evaporation of a drop of the appropriate tubule suspension on a Formvar grid provided samples for TEM analysis using an instrument described elsewhere.[11]

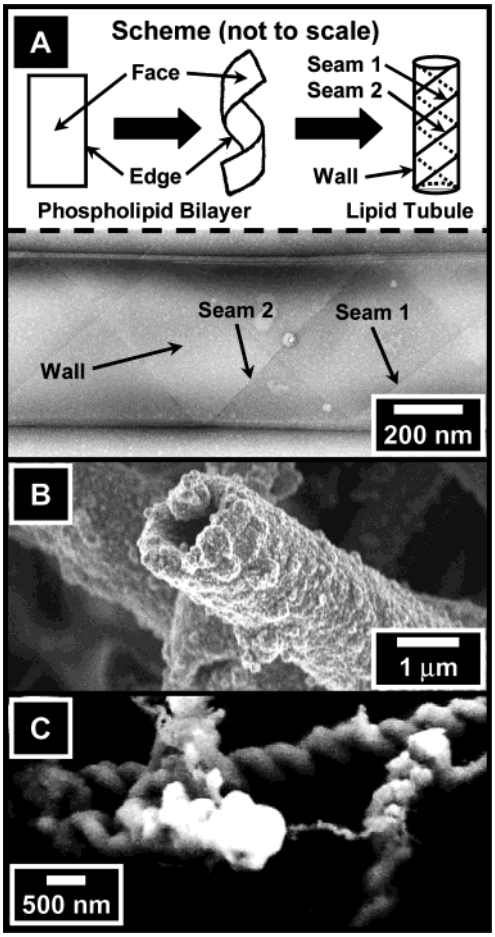

Figure 1. (A) Tubule formation scheme with a TEM image of a $DC_{8,9}PC$ microtubule stained with uranyl acetate showing the tubule structure; (B) TEM image of $DC_{8,9}PC$ microtubules completely coated by EL Cu following nonselective Pd/Sn catalysis according to the method of ref 11 (photo courtesy of M. Dinderman); (C) SEM image showing spiral EL Cu nanostructures formed after ~4 h plating of polyelectrolyte-coated $DC_{8,9}PC$ microtubules catalyzed by **PD3**.

Results and Discussion

The metallization templates used in our work are hollow microtubules and spiral structures prepared from chiral lipids, such as (L)-1,2-bis-(tricosa-10,12-diynoyl)-*sn*-glycero-3-phosphocholine ($DC_{8,9}PC$) or its analogues,[5,6] and self-assembled through thermal cycling or solvent-induced precipitation methods.[12,13] $DC_{8,9}PC$ microcylinders are produced as bilayer ribbons, initially formed in solution and driven by chiral interactions, spontaneously fold into hollow spiral structures much in the same way a paper soda straw is formed (Figure 1A, scheme).[14] The resulting microtubules typically average ~0.5 μm in width and range from a few to hundreds of micrometers in length.[11] Chiral architectures have been proposed and confirmed by circular dichroism studies,[15,16] and helical patterns marking the boundary seams of the folded lipid bilayers have been observed by transmission electron microscopy (TEM) inthe microtubule walls (Figure 1A), consistent with this formation mechanism.

$DC_{8,9}PC$ microtubules are readily metallized under ambient, aqueous conditions using standard EL processes.[11] Specifically,

(7) (a) Note that PSS is used as the first polyelectrolyte layer for adsorption to $DC_{8,9}PC$ tubule seams, whereas PEI is the first polyelectrolyte adsorbed to mixed $DC_{8,9}PEOH/DC_{8,9}PC$ tubules. For zwitterionic $DC_{8,9}PC$ tubules, the outermost cationic choline headgroup is presented at the tubule seam defects, requiring the use of negatively charged PSS polyelectrolyte for the first adsorption layer. Polyelectrolyte adsorption in this case is primarily driven by the strong flexoelectric field[7b,c,d,8] gradient naturally present at the seam defect sites, with weaker electrostatic attraction to the charge neutral, dipolar, phosphocholine groups. In contrast, concentration of the net negatively charged $DC_{8,9}PEOH$ lipid at the seam defects[8] in the mixed lipid tubules indicates the use of cationic PEI polyelectrolyte for the first adsorption layer. In this case, adsorption of the cationic PEI polymer occurs electrostatically to anionic phosphate headgroup sites of the $DC_{8,9}PEOH$ lipids via displacement of their mobile H^+ counterions. This adsorption mechanism supplements the contribution due to the naturally occurring flexoelectric field gradient at the seam defect sites, providing a potential pathway for more selective adsorption of larger amounts of polyelectrolyte at the $DC_{8,9}PEOH/DC_{8,9}PC$ tubule seams as required for improved catalysis and metallization. (b) The flexoelectric effect refers to the naturally occurring net radial electrostatic polarization present due to the curvature of the zwitterionic dipolar membrane of the tubule, as described in detail elsewhere.[7c,d,8] (c) Derzhanski, A.; Petrov, A. G.; Todorov, A. T.; Hristova, K. *Liq. Cryst.* **1990**, *7*, 439. (d) Petrov, A. G.; Spassova, M.; Fendler, J. H. *Thin Solid Films* **1996**, *285*, 845.

(8) Lvov, Y. M.; Price, R. R.; Selinger, J. V.; Singh, A.; Spector, M.; Schnur, J. *Langmuir* **2000**, *16*, 5932.

(9) Dressick, W. J.; Kondracki, L.; Chen, M.-S.; Brandow, S. L.; Matijević, E.; Calvert, J. M. *Colloids Surf., A* **1996**, *108*, 101.

(10) Koumoto, K.; Seo, S.; Sugiyama, T.; Seo, W. S.; Dressick, W. J. *Chem. Mater.* **1999**, *11*, 2305.

(11) Schnur, J. M.; Price, R.; Schoen, P.; Yager, P.; Calvert, J. M.; Georger, J.; Singh, A. *Thin Solid Films* **1987**, *152*, 181.

(12) Yager, P.; Schoen, P. E. *Mol. Cryst. Liq. Cryst.* **1984**, *106*, 371.

(13) Yager, P.; Schoen, P.; Georger, J.; Price, R.; Singh, A. *Biophys. J.* **1986**, *49*, 320A.

(14) Georger, J.; Singh, A.; Price, R.; Schnur, J.; Yager, P. *J. Am. Chem. Soc.* **1987**, *109*, 6169.

treatment of the tubule with a colloidal Pd/Sn catalyst leads to noncovalent catalyst adsorption at phospholipid sites. Subsequent immersion in an EL metal bath deposits a confluent metal film covering the surface of the tubule. The resulting hollow metal microstructures (Figure 1B) are useful as components for electroactive composites[17] and for controlled release applications.[18]

The fabrication of more complex structures, such as spiral metal features, requires the selective deposition of catalyst onto either the seam or the wall of the $DC_{8,9}PC$ microtubule in Figure 1A (i.e., the edge or the face, respectively, of the phospholipid ribbon comprising the tubule structure). For EL processes catalyzed by Pd/Sn, previous TEM studies indicate that the colloid adsorbs preferentially on the tubule seams.[11] However, because catalyst adsorption occurs via noncovalent van der Waals (and hydrogen-bonding) interactions, sufficient Pd is also adsorbed on the tubule walls to initiate metal deposition there as well, leading to complete (i.e., nonselective) metallization of the entire tubule surface.

Similar enhancements of binding capabilities at $DC_{8,9}PC$ tubule seams have also been noted during tubule interactions with other materials. For example, Burkett and Mann[19] attributed the formation of Au nanoparticles along helical seams of $DC_{8,9}$-PC tubules to Au(III) ion reduction by diacetylenic groups exposed at high surface energy bilayer edge defects there. Goren and co-workers[20] noted that charged pyrrole nuclei initially formed in solution were selectively adsorbed at $DC_{8,9}PC$ tubule seam defect sites via hydrophobic interactions, leading to formation of coiled polypyrrole strings and "necklaces" templated by the helical microstructure. In later work, Lvov and co-workers[8] suggested that large flexoelectric field[7b,c,d,8] gradients at tubule seams contribute to localized adsorption of charged materials at these sites. They demonstrated that polyelectrolyte multilayers could be preferentially adsorbed at the seams of $DC_{8,9}PC$ tubules containing small amounts of (L)-1,2-bis-(tricosa-10,12-diynoyl)-*sn*-glycero-3-phosphoethanol ($DC_{8,9}$-PEOH), a negatively charged lipid analogue of the zwitterionic $DC_{8,9}PC$ lipid in which an uncharged hydroxyl group replaces the cationic choline group. The ability of these tubules to form nanoparticle helices through electrostatic binding of charged silica colloids by the localized polyelectrolyte was attributed to the effective amplification of charge by the adsorbed polyelectrolyte and flexoelectric field gradients at the seams.

Given these observations, we postulated that it would be possible to induce selective EL metal deposition onto polyelectrolyte-coated tubule seams, provided that a catalyst that preferentially binds to the polyelectrolyte replaces the Pd/Sn colloid. It has been shown previously that negatively charged nanoparticles capable of functioning as EL catalysts (e.g., **PD1**)[9] can be prepared via condensation of chloro/hydroxy-based Pd(II) intermediates formed during $PdCl_4^{2-}$ hydrolysis. Although these nanoparticles typically bind covalently to surface ligand sites,[21,22] electrostatic binding to positively charged polyelectrolytes, such as poly(ethyleneimine) (PEI), can also occur. Therefore, we sequentially treated $DC_{8,9}PC$ microtubules with PSS (i.e., sodium polystyrenesulfonate), PEI, PSS, and PEI solutions, using multiple centrifugations to separate the tubules from unadsorbed polyelectrolyte in solution after each step.[8] Afterward, the negatively charged **PD1** nanoparticle catalyst[9] was electrostatically adsorbed to the outermost cationic PEI layer of the PSS/PEI/PSS/PEI multilayer coating the tubule seams. Unfortunately, EL Cu deposition proceeded incompletely on these tubules, with no clear evidence for selective, templated, metal deposition at the tubule seams.

The poor metallization behavior observed was eventually traced to two sources. First, the literature **PD1** nanoparticle EL catalyst[9] apparently contained insufficient Pd(II) to completely catalyze the high surface area, polyelectrolyte-coated, tubule seams. Second, metallization of polyelectrolyte-lipid debris, created due to tubule fragmentation during the numerous centrifugations and washings associated with multilayer deposition, hindered our observation of any templated metal nanostructures. Therefore, we prepared a modified catalyst, designated **PD3**, by increasing the Pd(II) level of the literature **PD1** catalyst[9] ~10-fold (note Experimental Section). In addition, we titrated the tubules with PEI and PSS to estimate the minimum amounts of each solution required for complete polyelectrolyte adsorption during each cycle, thereby eliminating the need to separate tubules from solution containing excess, unadsorbed polyelectrolyte after each deposition cycle (note Experimental Section).

Using the **PD3** formulation and these modified polyelectrolyte deposition procedures, we obtain spiral metal nanostructures (Figure 1C) during Cu deposition, consistent with a templated metallization process and the chirality of the underlying $DC_{8,9}$-PC lipid.[23] Although well-formed spiral Cu structures are now observed, agglomerated, distorted, and irregular-shaped metal objects still comprise a majority of the metal product.[24] The percentage of polyelectrolyte-treated $DC_{8,9}PC$ tubules yielding well-formed spiral Cu structures varies with different tubule batches, ranging from nearly zero to ~20%, and correlates with tubule surface structure. Specifically, tubules exhibiting well-defined seams, as shown in Figure 1A, generally yield larger fractions of spiral Cu structures than tubules whose seams have annealed and are therefore less prominent. Such behavior is consistent with previous arguments concerning the presence of defect sites and associated regions of enhanced flexoelectric field gradient as prerequisites for the preferential adsorption of species to the tubules.[8,19,20]

Our observations concerning the formation of the $DC_{8,9}PC$ templated spiral Cu features suggest that control of factors affecting tubule structure, such as lipid composition and chemistry or temperature gradient during tubule preparation, should allow us to optimize the preferential polyelectrolyte

(15) Selinger, J. V.; MacKintosh, F. C.; Schnur, J. M. *Phys. Rev. E: Stat. Phys., Plasmas, Fluids, Relat. Interdiscip. Top.* **1996**, *53*, 3804.
(16) Spector, M. S.; Easwaran, K. R. K.; Joythi, G.; Selinger, J. V.; Singh, A.; Schnur, J. M. *Proc. Natl. Acad. Sci. U.S.A.* **1996**, *93*, 12943.
(17) Browning, S. L.; Lodge, J.; Price, R. R.; Schelleng, J.; Schoen, P. E.; Zabetakis, D. *J. Appl. Phys.* **1998**, *54*, 6109.
(18) Price, R.; Patchan, M. *J. Microencapsulation* **1991**, *8*, 301.
(19) Burkett, S. L.; Mann, S. *Chem. Commun.* **1996**, 321.
(20) Goren, M.; Zhigang, Q.; Lennox, R. *Chem. Mater.* **2000**, *12*, 1222.
(21) Dressick, W. J.; Dulcey, C. S.; Georger, J. H., Jr.; Calabrese, G. S.; Calvert, J. M. *J. Electrochem. Soc.* **1994**, *141*, 210.
(22) Brandow, S. L.; Chen, M.-S.; Wang, T.; Dulcey, C. S.; Calvert, J. M.; Bohland, J.; Calabrese, G. S.; Dressick, W. J. *J. Electrochem. Soc.* **1997**, *144*, 3425.
(23) All Cu spiral structures shown in the figures exhibit the same handedness (in this case, right-handed spirals), as expected given our use of the lipid L-enantiomers to prepare tubule templates.
(24) The presence of agglomerates and irregular metal particles is consistent with any one or more of the following scenarios: (1) bridging of adjacent tubules by polyelectrolyte during its deposition; (2) binding of polyelectrolyte layers on two or more tubules by a single nanoparticle catalyst; (3) fragmentation of catalyzed tubules during centrifugation; (4) isolation of larger, unbound catalyst particles together with catalyzed tubules during centrifugation. We are unable to discern the relative contributions of these factors given our current data.

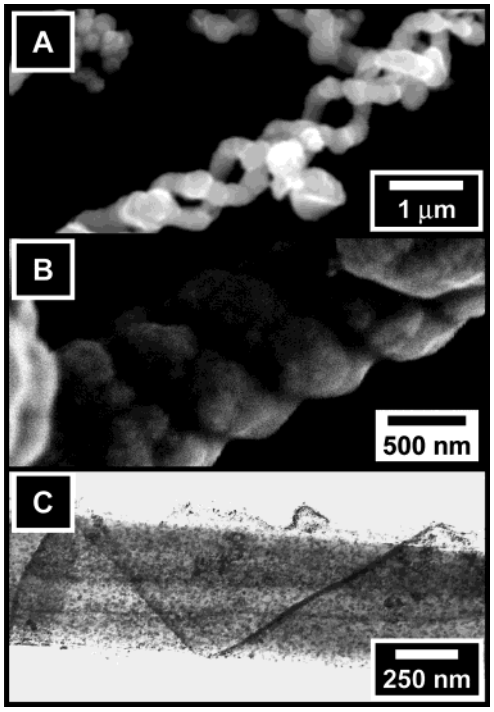

Figure 2. (A) SEM image of an isolated spiral Cu structure formed after ~2 h Cu EL plating of the polyelectrolyte-coated $DC_{8,9}PEOH/DC_{8,9}PC$ tubules catalyzed by **PD3**; (B) SEM image of a spiral Cu structure formed on polyelectrolyte-coated $DC_{8,9}PEOH/DC_{8,9}PC$ tubules catalyzed by **PD3** after ~5 h Cu plating; (C) TEM image of $DC_{8,9}PEOH/DC_{8,9}PC$ tubules coated with PEI/PSS/PEI polyelectrolyte film after **PD3** catalysis. The darkened areas indicate the binding of Pd(II).

binding at tubule seams required to improve the yield of spiral Cu structures. Therefore, we examined the effect of lipid composition on the formation of spiral Cu structures to test this hypothesis. In this case, we used mixed lipid tubules prepared from zwitterionic $DC_{8,9}PC$ lipid doped with the negatively charged $DC_{8,9}PEOH$ lipid (2 wt %). Enhanced concentration of the negatively charged $DC_{8,9}PEOH$ lipid at the tubule seams under the influence of the high flexoelectric field gradient present at such defect sites is predicted to occur during tubule formation,[8] effectively establishing and amplifying a fixed net negative charge at the tubule seams. Consequently, it is expected that both the quantity of charged polyelectrolyte and its preference for adsorption at the seams will be enhanced for the mixed lipid tubules as compared to the pure $DC_{8,9}PC$ tubules, permitting more selective binding of larger amounts of catalyst required for fabrication of the spiral metal structures in higher yields and in a more reproducible manner. These expectations are borne out in Figure 2A and 2B, which show SEM images of mixed lipid tubules sequentially treated with PEI, PSS, and PEI,[7] catalyzed using **PD3**, and plated with Cu. The yield of intact spiral Cu features averages ~30% for the mixed lipid tubules, and batch-to-batch reproducibility (i.e., ~25−40%) is somewhat improved as compared to the pure $DC_{8,9}PC$ system.

The formation of Cu spiral structures in Figures 1C, 2A, and 2B also depends on the total number of polyelectrolyte layers deposited onto the tubule seams. The number of polyelectrolyte layers sufficient for spiral fabrication is 3 for the mixed $DC_{8,9}PEOH/DC_{8,9}PC$ tubules and 4 for the pure $DC_{8,9}PC$ tubules, with a terminal PEI layer present in both cases for catalyst binding. Metallization template quality is compromised, and unequivocal evidence for formation of Cu spiral structures is absent when fewer polyelectrolyte layers are present. A tendency for nonselective overplating, leading eventually to complete coating of the tubule by Cu metal similar to Figure 1B, is observed as the number of polyelectrolyte layers deposited increases.

The fidelity of the metallization process, as measured by the uniformity of well-formed Cu spirals in Figures 1C and 2B, is not greatly influenced by the slight differences in lipid composition of the tubules used in our experiments. For example, a pitch angle of ~48 ± 9° is observed for the spiral Cu structures formed using either the $DC_{8,9}PC$ or the mixed $DC_{8,9}PEOH/DC_{8,9}PC$ tubule templates. This angle is identical within experimental error to the pitch angle of 42 ± 6° routinely observed for ~0.5 μm diameter $DC_{8,9}PC$ tubules (Figure 1A).[8] This relationship is observed even as the plated Cu thickness is increased in Figure 2B to the point where fusion of Cu from segments of the adjacent spirals occurs. This behavior suggests that the tubule template is not significantly distorted during the deposition of the polyelectrolyte, catalyst, and Cu metal and that mechanical distortions in the Cu spiral features observed in Figures 1C and 2A are likely introduced during the handling and preparation of the samples for SEM imaging.

The susceptibility of the spiral Cu structures to mechanical deformation during handling is hardly surprising, given the dimensions of the free-standing metal features. Measurements of individual coil widths[10] of the Cu spirals yield average widths of just ~423 ± 28, ~339 ± 56, and ~561 ± 30 nm, respectively, for the structures of Figures 1C, 2A, and 2B (~50 measurements each). The larger standard deviation relative to feature width noted in Figure 2A reflects the shorter plating time for this sample (~2 h) as compared to that for Figures 1C (~4 h) or 2B (~5 h). In Figure 2A, individual Cu particles grown from catalyst nucleation sites along the tubule seam have recently fused to complete the spiral structure and are still barely visible. However, sufficient Cu has not yet been deposited at the junctions between the particles to increase the thickness of the metal strand there, leading to the observed variation in feature width. Lateral growth of Cu along the direction of the seam occurs with increased plating times, ultimately providing structures with good feature definition and uniformity, as shown in Figures 1C and 2B. This behavior contrasts markedly with the large feature width variations observed for $DC_{8,9}PC$ tubule-templated polypyrrole threads prepared by Goren and co-workers.[20]

The contrast between the morphology of our Cu spirals and Goren's[20] polypyrrole strands reflects fundamental differences in the deposition mechanisms in the two systems. For the templated polypyrrole strands, charged pyrrole nuclei initially formed in solution are adsorbed at defect sites in the tubule seam, where they catalyze polymerization to form templated strands. Growth of nuclei also occurs simultaneously in the aqueous solution with subsequent adsorption and incorporation of these larger particles into the templated polymer strands on the tubule seams. As a result, the width of the polymer strand varies in those regions where such particles are incorporated, leading to a "necklace" morphology.

In our case, catalyst particles are prebound onto the polyelectrolyte adsorbed on the tubule seams. Because EL metal deposition occurs under conditions where there are no catalyst particles remaining in solution, competitive metal nucleation and growth in solution with subsequent adsorption of metal particles onto the tubule template cannot occur. However, this

factor alone is not sufficient to explain the relatively smooth and uniform metal deposits we observe. Catalysts such as **PD1** and **PD3** are comprised of nanoparticles having a wide range of sizes.[9] Because metal growth rates scale with the size of the catalyst particle,[25] equal binding of all members of the distribution would lead to a broad distribution of metal particle sizes in the metal film, resulting in a correspondingly rough surface contrary to our observations in Figures 1C, 2A, and 2B.

It is well known that when lower densities of ligating sites are present on surfaces, the ligands can preferentially bind a narrow size range of catalyst particles within the broader particle distribution, leading to a smoother morphology for the subsequent EL metal deposit.[25,26] For example, **PD1** catalyst dispersion contains particles ranging in diameter from $< \sim 4$ to ~ 53 nm.[21] When an aminosiloxane monolayer coating a Si wafer is UV irradiated to destroy 90% of the amine ligand binding sites, the remaining amines preferentially bind nanoparticles having sizes ≤ 10 nm from the **PD1** dispersion.[25] Polyvinylpyridine films adsorbed onto TEM Cu grids also exhibit a preference for binding **PD1** nanoparticles of diameter $\sim 5-10$ nm.[25] Consequently, we examined polyelectrolyte-coated tubules catalyzed by **PD3** prior to Cu deposition to determine whether size-selective binding of catalyst nanoparticles contributes to the formation of smooth, uniform Cu structures in our systems.

Figure 2C shows a TEM image of a polyelectrolyte-coated mixed lipid microtubule following treatment with **PD3** in which darkened regions indicate Pd(II) binding. The image clearly indicates that Pd(II) is bound over the entire surface of the microtubule. However, particles are bound at higher densities on the tubule seams than on the walls, consistent with localized polyelectrolyte binding at the high-energy seams. Particle sizes bound to the polyelectrolyte at the seams range from $< \sim 3$ to ~ 6 nm in diameter (75 measurements), confirming that size-selective binding of catalyst does occur in our systems. The catalyzed seam boundaries appear smooth and continuous, as expected given the narrow size range of bound particles and as required to obtain the uniform Cu spirals. In control experiments (not shown), catalyst particle binding similar to that observed on the tubule walls in Figure 2C was noted upon treating tubules not coated by polyelectrolyte with **PD3**. However, these control tubules failed to metallize reproducibly in the Cu EL bath.

The TEM experiments are consistent with our metallization model and the previously documented behavior of the EL catalysts.[9,21,22,25] For the catalysts, a minimum bound surface concentration of $\sim 10^{15}$ Pd(II) sites/cm^2 is required to initiate and sustain EL metal deposition.[21] The binding of negatively charged catalyst onto lipid sites on control $DC_{8,9}PC$ microtubules (not treated with polyelectrolyte) can only occur due to favorable, weak, electrostatic interactions with the charge neutral, dipolar, phosphocholine sites of the lipid headgroups because there are no covalent ligating sites present. Electrostatic and steric arguments suggest that, in this case, selective binding of smaller, less negatively charged catalyst particles is favored at the expense of larger, more highly charged particles in the catalyst dispersion.[25] In fact, catalyst binding behavior on the control $DC_{8,9}PC$ tubules is similar to that observed for the tubule walls (i.e., areas not coated by polyelectrolyte) in Figure 2C; that is, only the smaller catalyst particles having diameters $< \sim 8$ nm within the **PD3** dispersion are bound, consistent with these arguments. Although catalyst can be bound under these conditions, apparently an insufficient quantity to reproducibly initiate and sustain EL Cu deposition is present on the control $DC_{8,9}$-PC tubule seams and walls in this case.

In contrast, the ability to metallize the polyelectrolyte-coated tubules, as shown in Figures 1C, 2A, and 2B, shows that sufficient Pd(II) is bound in these cases to initiate Cu deposition. This indicates that Cu deposition must initiate at the tubule seams, given the higher density of bound Pd(II) observed there than on the tubule walls in Figure 2C. The question of whether there is also sufficient Pd(II) bound on the tubule walls to initiate metallization there as well cannot be answered using Figure 2C in the absence of information relating Pd(II) image density to surface Pd(II) concentrations. However, the observation of intertwined Cu spirals in Figure 2A is clearly inconsistent with initiation of Cu deposition on the tubule walls. Such a process, if it occurred, would simultaneously bridge the metal growth initiated at each seam and would be expected to produce a metal ribbon structure similar in shape to the twisted bilayer shown in Figure 1A, scheme. Consequently, Cu deposition initiates only at the tubule seams and eventually spreads over the surface of the tubule wall to produce the spiral structures shown in Figures 1C and 2B, consistent with previous studies and models indicating preferential materials binding at the seam sites.[8,19,20]

Conclusions

In conclusion, we have demonstrated a method for the fabrication of spiral metal structures having nanoscale dimensions using a phospholipid microtubule as a metallization template. The method relies on the use of preferentially adsorbed polyelectrolytes to create and amplify the ligand sites required to electrostatically bind a negatively charged EL metallization catalyst at naturally occurring seams present in the microtubules. Although we have demonstrated the use of Cu to form these nanostructures, the possibility exists to utilize other metals such as Co, Ni, Fe, Ag, Au, or their alloys[27] to vary the magnetic, electrical, chemical, and physical properties of the resulting structures. In a similar fashion, through controlled modification of the chemical structures of the lipids[5,6,28] comprising the microtubules, the translation of changes in pitch, chirality, and physical dimensions of the template into corresponding metal nanostructures is anticipated. We are currently exploring these possibilities to fabricate nanosprings, inductors, and conductors for use in applications involving electronics and composite materials.

Acknowledgment. The authors gratefully acknowledge financial support for this work from the Office of Naval Research through an internal 6.2 level research grant from the U.S. Naval Research Laboratory core-funding program.

Note Added after ASAP. The version posted on 8/15/2003 was the uncorrected version and contained errors in the scientific content. The version published 8/15/2003 and the print version are correct.

JA036173G

(25) Brandow, S. L.; Dressick, W. J.; Marrian, C. R. K.; Chow, G.-M.; Calvert, J. M. *J. Electrochem. Soc.* **1995**, *142*, 2233.
(26) Kim, J. U.; O'Shaughnessy, B. *Phys. Rev. Lett.* **2002**, *89*, 238301.
(27) *Electroless Plating: Fundamentals and Applications*; Mallory, G. O., Hajdu, J. B., Eds.; American Electroplaters and Surface Finishers Society: Orlando, FL, 1990; Chapters 1, 10, 15−18 and references therein.
(28) Singh, A.; Wong, E. M.; Schnur, J. M. *Langmuir* **2003**, *19*, 1888.